Carbohydrate Polymers 229 (2020) 115452

Contents lists available at ScienceDirect

Carbohydrate Polymers

journal homepage: www.elsevier.com/locate/carbpol

Revisiting very disperse macromolecule populations in hydrodynamic and light scattering studies of sodium carboxymethyl celluloses

Mandy Grube[a,b], Igor Perevyazko[c], Thomas Heinze[a,b], Ulrich S. Schubert[a,b], Ivo Nischang[a,b,*]

[a] Laboratory of Organic and Macromolecular Chemistry (IOMC), Friedrich Schiller University Jena, Humboldtstraße 10, 07743, Jena, Germany
[b] Jena Center for Soft Matter (JCSM), Friedrich Schiller University Jena, Philosophenweg 7, 07743, Jena, Germany
[c] Department of Molecular Biophysics and Physics of Polymers, St. Petersburg State University St. Petersburg, 7/9 Universitetskaya nab., St. Petersburg, 199034, Russian Federation

ARTICLE INFO

Keywords:
Absolute molar mass
Analytical ultracentrifugation
Conformation
Diffusion
Dispersity
Hydrodynamic invariants
Light scattering
Macromolecular chain properties
Rotational friction
Translational friction

ABSTRACT

One of the most abundant natural macromolecule, cellulose, is of high importance in technological research including medicine, energy application platforms, and many more. One of its most important ionic derivatives, sodium carboxymethyl cellulose, is known to be very disperse and heterogeneous. The experimental robustness of the methods of hydrodynamics and light scattering are put to test by studying these highly disperse, charged, and heterogeneous macromolecule populations. The following opportunities for molar mass estimations from experimental data were taken into consideration: (i) from the classical Svedberg equation, (ii) from size exclusion chromatography coupled to multi-angle laser light scattering, (iii) from the hydrodynamic invariant, and (iv) the sedimentation parameter. The orthogonality of such approach demonstrates a statistically robust assessment of chain conformational and chain dimensional characteristics of macromolecule populations. Quantitative comparison between the absolute techniques indicates that those have to be checked for accuracy of the obtained and derived characteristics.

1. Introduction

Renewable raw materials find a growing interest, especially because they can partially replace the becoming scarcer fossil raw materials. Besides renewable raw materials have important benefits such as ecologically important CO_2 neutrality, the possibility for the production of bio-based, biodegradable, and / or bio-compatible polymers or the extraction of chemicals with defined stereo-chemical structure. Carbohydrates are one of the most important classes of renewable raw materials (Lichtenthaler & Peters, 2004; Lichtenthaler, 2007; Nasatto et al., 2015; Ramesh & Tharanathan, 2003). The main proponent of carbohydrates, cellulose, has always been an essential commercial material such as wood, textiles, etc (Klemm, Heublein, Fink, & Bohn, 2005). Due to the possibility of its chemical derivatization, it occupies an important place in the economy as an industrial material. The commercial production of cellulose in Germany started in the early 1920s (Hollabaugh, Burt, & Walsh, 1945).

Carboxymethyl celluloses (CMCs) are commercially produced of cellulose activated with aqueous sodium hydroxide applying monochloroacetic acid or its sodium salt as reagent (Heinze & Koschella, 2005; Heinze & Pfeiffer, 1999). The products obtained in this process are supposed to be heterogeneous in terms of chemical composition and molar mass (Saake et al., 2000). Thus, in order to obtain information on the influence of the molecular structure of CMCs for applicative purposes, not only their average chemical composition and molar mass need to be known, but of particular consideration is the extend of respective dispersities / heterogeneities and their impact on overall materials properties.

CMC is the most important ionic cellulose ether. Through its hydrophilicity, CMC is also biocompatible. The viscous solutions of CMC in water have the advantage of thickening, suspending, and stabilizing properties, also in conjunction with other colloids. Such solutions allow access to form tough films upon solvent evaporation (Hollabaugh et al., 1945). Other applications of CMC concern its use as binding agent in thin layer batteries (Lee & Oh, 2013; Li, Lewis, & Dahn, 2007; Luna-Martínez et al., 2011). CMC is a “green” compound compared to polyvinylidene fluoride that is used in related applications (Kim et al., 2011). Further application fields can be found in the pharmaceutical and medical sciences (Nadagouda & Varma, 2007). CMCs can act as carrier material in drug delivery systems (Aravamudhan, Ramos, Nada,

* Corresponding author at: Laboratory of Organic and Macromolecular Chemistry (IOMC), Friedrich Schiller University Jena, Humboldtstraße 10, 07743, Jena, Germany.
E-mail address: ivo.nischang@uni-jena.de (I. Nischang).

https://doi.org/10.1016/j.carbpol.2019.115452
Received 24 July 2019; Received in revised form 26 September 2019; Accepted 5 October 2019
Available online 11 October 2019
0144-8617/

& Kumbar, 2014; El-Hag Ali, Abd El-Rehim, Kamal, & Hegazy, 2008; Li, Song, & Seville, 2010). Particularly here, an exact characterization and knowledge of its molecular properties is of pivotal importance to establish quantitative structure-property relationships and for quality control purposes.

The methods of molecular hydrodynamics (Lebowitz, Lewis, & Schuck, 2002; Svedberg & Sjögren, 1930) and light scattering (Debye, 1947; Wyatt, 1993) are widely applied in macromolecular characterization to assess solution properties of synthetic- and bio-macromolecules. In this context, these powerful and eminent methods are most insightful when studying very well-defined samples such as proteins and their aggregates. These methods as well have been shown useful when studying synthetic macromolecules of narrow dispersity that are available by contemporary precision synthesis utilizing reactions of, e.g., a living nature (Grube, Leiske, Schubert, & Nischang, 2018; Nischang et al., 2017), including their conjugates to (bio-)macromolecules (Lühmann et al., 2017). Notwithstanding, studies concerning samples featuring very disperse and even multimodal molar mass distributions, reconciled by analysts depending on the degree of resolution available by particular techniques, are scarce and require attention. The inherent drawback of solution characterization of very disperse and heterogeneous samples, therefore, is considered the "holy grail" in demonstrating the power of solution characterization through hydrodynamics and light scattering. Also, frequently only one of these absolute techniques is considered or available (Harding et al., 2015; Oberlerchner, Rosenau, & Potthast, 2015; Sitaramaiah & Goring, 1962).

In this study, we test the conceptual opportunity of the methods of molecular hydrodynamics (solution viscometry, sedimentation velocity experiments, diffusion measurements) on very disperse CMCs that, in addition to their dispersity and potential heterogeneity, carry an anionic charge density in aqueous sodium chloride. The CMCs are also characterized by evaluating their degree of substitution (DS) by high performance liquid chromatography (Heinze, Erler, Nehls, & Klemm, 1994) in order for allowing substantiated conclusions concerning their behavior and conformational characteristics in solution.

Next to the reported primary data concerning hydrodynamic measurements performed under translational (sedimentation, diffusion) and rotational (viscometry) friction in aqueous sodium chloride, we also report size exclusion chromatography measurements coupled to multi-angle laser light scattering (SEC-MALLS) experiments in the same aqueous sodium chloride solvent for independent molar mass estimations. The complex set of data allows for the interrelation of all average macromolecular characteristics through the concept of the hydrodynamic invariant and the sedimentation parameter. Along this line, we also focus on the core question of the most meaningful value of average molar masses, characterizing this set of macromolecules in concert with their fundamental macromolecular chain characteristics.

2. Experimental

2.1. Materials

All CMCs were purchased from Sigma Aldrich. All experiments were performed in 0.1 M aqueous sodium chloride ($\varrho_0 = 1.0024\,g\,cm^{-3}$, $\eta_0 = 1.0062\,mPas$). The pH-value of the CMC solutions was determined to be 6.8 ± 0.1. The water content was determined to be within 3.9 to 7.5 % (Table S1). Further experimental details can be found in the Supporting Information. The degree of substitution (DS) was determined by high performance liquid chromatography as described previously (Heinze et al., 1994). In Fig. S1, liquid chromatographic measurements from all CMCs are shown and results listed in Table S1. The presence of sodium chloride salts was checked for as detailed in the Supporting Information.

These preliminary experimental considerations indicate that different molar mass samples could be compared via the variety of techniques utilized in this manuscript, keeping in mind that the potential impact of varying salt concentration for the samples may lead to different specific estimates due to conformational variations of the macromolecules. In fact, the same mass of macromolecules, irrespective of their molar mass, provides the approximately same total amount of charged moieties present in solution, just that a different number of such macromolecules is present due to the different molar masses and individual dispersities / heterogeneities.

2.2. Viscometry

For the determination of the intrinsic viscosities, $[\eta]$, we followed literature procedures from our previous work (Grube et al., 2018; Nischang et al., 2017). The intrinsic viscosity, $[\eta]$, was determined via both the Huggins- and Kraemer relations (Eqs. (S1) and (S2)). A detailed description of the adapted literature procedure and instrument details can be found in the Supporting Information.

2.3. Partial specific volume

Partial specific volumes, υ, were determined according to the procedures described recently (Grube et al., 2018; Nischang et al., 2017). A detailed description of the adapted literature procedure can be found in the Supporting Information. The determined value is $\upsilon = 0.55 \pm 0.01\,cm^3\,g^{-1}$ (Fig. S2).

2.4. Sedimentation velocity / synthetic boundary experiments

Sedimentation velocity / synthetic boundary experiments were performed using a ProteomeLab XL-I analytical ultracentrifuge (Beckman Coulter Instruments, Brea, CA) with an An-50 Ti eight-hole rotor, using double-sector epon centerpieces with a 12 mm optical path length. An in-depth description of these experiments together with the put-forward details on data analysis can be found in the Supporting Information.

2.5. Size exclusion chromatography coupled to multi-angle laser light scattering (SEC-MALLS)

Measurements were performed on an adapted asymmetrical flow field-flow fractionation instrument (AF2000 MT) from Postnova Analytics GmbH (Landsberg, Germany) as described previously (Grube et al., 2018). Experimental details and determination of the refractive index increment (Fig. S3) can be found in the Supporting Information. Control experiments of similarity between filtered and non-filtered samples investigated can be found in Fig. S4 of the Supporting Information.

3. Results and discussions

The fundamental key problem addressed in this work is to establish a correlation between the chemical structure of the macromolecules (Scheme 1) and its particular solution properties in aqueous sodium chloride.

A perhaps classical way in determining such structure-property relationships in solution is a direct investigation of the corresponding molecular and conformational characteristics of macromolecules. The success of such investigations depends on the overall complexity of the macromolecular system being studied. This complexity will be

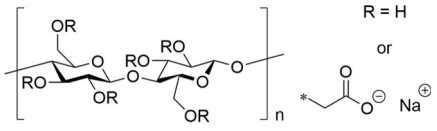

Scheme 1. Schematic representation of sodium carboxymethyl cellulose (CMC).

determined in particular by the molecular architecture, presence of charged moieties, solvent-solute interactions and dispersity / heterogeneity of the population of macromolecules. The CMCs are a particularly well-suited example of highly disperse, charged (bio-)macromolecules and, as a consequence, difficult to study. Though several studies using a variety of solvents are available in the literature (Arinaitwe & Pawlik, 2014; Brown & Henley, 1964; Murodov, Urinov, & Turaev, 2018; Lavrenko, Okatova, Dauttsenberg, & Filipp, 1991; Lavrenko, Okatova, & Dautzenberg, 1999; Pohl, Morris, Harding, & Heinze, 2009; Rinaudo, Danhelka, & Milas, 1993; Shakun, Maier, Heinze, Kilz, & Radke, 2013; Sitaramaiah & Goring, 1962), these have not been compared against each other and checked for their consistency. One of the best possible approaches is to use a combination of complementary hydrodynamic and light scattering methods.

At first, we approach this issue by discussing primary hydrodynamic experimental data performed under rotational (viscosity) and translational (sedimentation and diffusion) friction as well as separation and light scattering experimental data, keeping in mind the inherent dispersity of the macromolecules. These primary data are then interrelated and checked for their consistency by the hydrodynamic invariant and sedimentation parameter. Afterward, we move to the evaluation of the molar masses by sedimentation-diffusion analysis through sedimentation velocity experiments in the ultracentrifuge, respectively, determination of diffusion coefficients decoupled from sedimentation through synthetic boundary experiments. Finally, we compare molar mass results from hydrodynamic studies to the ones determined independently using SEC-MALLS under the same solution conditions. We as well utilize the hydrodynamic invariant concept and sedimentation parameter in molar mass estimations, particularly where inconsistencies of a particular method were evident. Consequently, and despite their very high dispersity / heterogeneity, we will provide a corresponding conformational analysis of the CMCs in solution by statistically most relevant values of the obtained molar masses from all techniques presented.

3.1. Rotational and translational friction

The following hydrodynamic characteristics are of prime importance – intrinsic viscosities, $[\eta]$ (Eq. (1)), sedimentation coefficients at infinite dilution, s_0 (Eq. (2)), and translational diffusion coefficients at infinite dilution, D_0 (Eq. (3)):

$$[\eta] = \Phi\frac{<h^2>^{3/2}}{M} \tag{1}$$

$$s_0 = \frac{M(1-\upsilon\varrho_0)}{N_A P\eta_0 <h^2>^{1/2}} \tag{2}$$

$$D_0 = \frac{k_B T}{P\eta_0 <h^2>^{1/2}} \tag{3}$$

where Φ and P are Flory hydrodynamic parameters that are functions of L/A and d/A with L being the contour length of the macromolecule, A being the Kuhn segment length, and d being the diameter of the macromolecular chains. $<h^2>$ is the mean square end-to-end distance of the macromolecular chain, M is the molar mass, k_B is the Boltzmann constant, N_A is the Avogadro number, and T is the absolute temperature.

3.2. Rotational friction – viscometry

Fig. 1 shows Huggins viscosity plots for all investigated CMC samples. Fig. S5 includes Kraemer plots as well. The intrinsic viscosity, $[\eta]$, is very sensitive to size variations (Eq. (1)), thereby linearity of the experimental viscometry dependences (Figs. 1 and S5) indicates the absence of major macromolecular backbone charge effects.

The CMCs studied are displaying a broad range of intrinsic viscosities from $[\eta] \approx 170\, cm^3 g^{-1}$ for CMC 1 up to $[\eta] \approx 1700\, cm^3 g^{-1}$ for CMC 10, i.e. an order of magnitude. The Huggins, k_H, and Kraemer, k_K, viscometric constants are shown in Table S2 and demonstrate that the different samples do not vary in their interaction with the solvent.

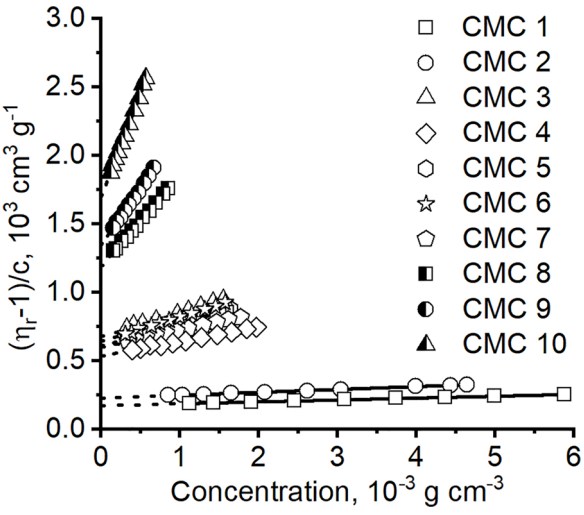

Fig. 1. Huggins extrapolation plots for the determination of the intrinsic viscosities, $[\eta]$, for all CMC samples in 0.1 M aqueous sodium chloride at a temperature of $T = 20.0\,°C$.

The product of intrinsic viscosity, $[\eta]$ in $cm^3 g^{-1}$, and concentration in units $g\, cm^{-3}$ represents the volume fraction of macromolecular chains in solution, a practically used dimensionless value to define the degree of dilution, the so-called Debye parameter (Pavlov, Perevyazko, Okatova, & Schubert, 2011):

$$\varphi \equiv \frac{n\nu}{V} = \frac{m\nu N_A}{VM} = \frac{c0.36 <h^2>^{3/2} N_A}{M} = (\frac{0.36 N_A}{\Phi})c[\eta] \approx c[\eta] \tag{4}$$

where n is the number of macromolecules in a certain volume, V, ν is the volume occupied by a macromolecular chain, and m refers to the mass of the macromolecule in a volume, V. Together with the definition of the intrinsic viscosity, $[\eta]$, (Eq. (1)) the volume occupied by macromolecules in solution may roughly be approximated by $c[\eta]$ (right hand side of Eq. (4)). If $c[\eta] \ll 1$ the corresponding solution can be considered as dilute, i.e., no overlap of macromolecular structures occurs.

3.3. Translational friction I – sedimentation

An empirical description of sedimentation boundaries and their derivatives, while discussing the boundary-sharpening (Fujita, 1956) and Johnston-Ogston effect (Chaturvedi, Ma, Brown, Zhao, & Schuck, 2018; Johnston & Ogston, 1946), depending on the degree of dilution, can be found in the Supporting Information (Fig. S6). Fig. 2 shows examples of differential distributions of sedimentation coefficients from the $c(s)$ model incorporated in Sedfit and respective concentration dependences. Experimentally, the sedimentation velocity experiments were performed in a wide range of concentrations of the corresponding macromolecule solutions from dilute to semi-dilute, and concentrated ($0.01 < c[\eta] < 6$, Eq. (4)). At macromolecule concentrations of $c = 3 \times 10^{-3} g cm^{-3}$, corresponding to the dilute regime for CMC 1 ($c[\eta] = 0.5$, Eq. (4)), the bimodal distribution appears readily narrow. However, at more than an order of magnitude lower concentration of $c = 0.1\, x\, 10^{-3}\, g\, cm^{-3}$, corresponding to the highly dilute regime ($c[\eta] = 0.02$), the bimodal distribution appears to feature a much wider distribution of sedimentation coefficients (Fig. 2a). A similar situation with even more developed multimodality at high degrees of dilution was revealed for the CMC 10. In this case as well, the ls-g*(s) model without considering effects of diffusion envelopes the c(s) model (see dashed lines in Fig. 2c). The high molar mass sample occupies a much larger molecular volume in solution, and therefore resembles a

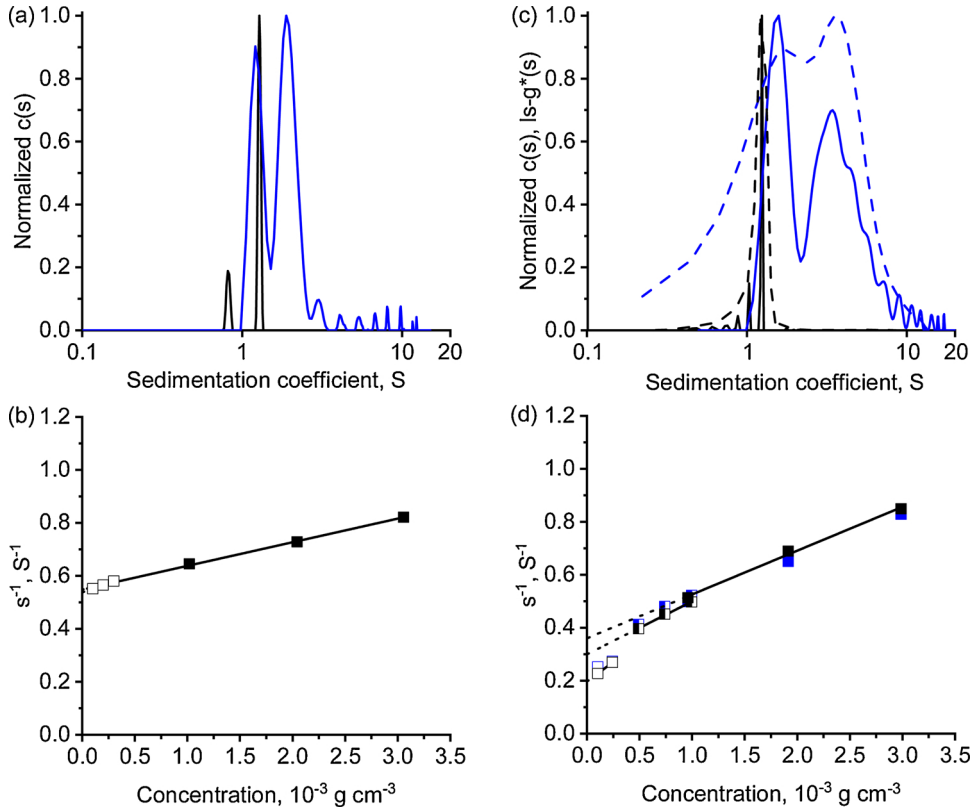

Fig. 2. Normalized differential distributions of sedimentation coefficients $c(s)$ (solid lines) of (a) CMC 1 and (c) CMC 10 on a semi-logarithmic scale at $c = 3 \times 10^{-3} g cm^{-3}$ (black lines) and $c = 0.1 \times 10^{-3} g cm^{-3}$ (blue lines). For CMC 10, also the $ls - g^*(s)$ model (dashed lines in (c)) at the respective concentrations is shown. Concentration dependence of the inverse sedimentation coefficients, s^{-1} (Eq. (S4)), are shown for (b) CMC 1 and (d) CMC 10. Open, half-filled, and filled squares highlight the different degrees of dilution. The solid lines refer to linear fits, while the dotted lines refer to extrapolations (Eq. (S4)). (d) Contains data from the $ls - g^*(s)$ model shown with blue symbols as well. Experiments were all performed in 0.1 M aqueous sodium chloride at a temperature of $T = 20.0\,°C$. (For interpretation of the references to colour in this figure legend, the reader is referred to the web version of this article).

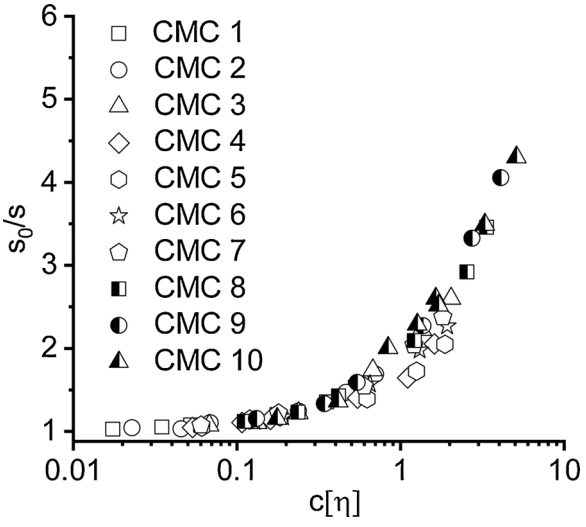

Fig. 3. Semi-logarithmic plot of s_0/s against $c[\eta]$ for CMCs 1–10 in 0.1 M aqueous sodium chloride at a temperature of $T = 20.0\,°C$.

completely different degree of dilution, $c[\eta]$ (Eq. (4)), within the same concentration range as studied for the CMC 1. These observations are clearly reflected already in the empirical description of the differentials of the sedimentation boundaries described in the Supporting Information (Fig. S6).

In the following analysis weight (signal) averages of the distributions, being multimodal or not, were utilized by integrating over the entire differential distributions of sedimentation coefficients. This approach was chosen, because it is generally considered necessary to take an average of the entirety of the sedimentation coefficient populations for further considerations. In case of CMC 10 as well, the agreement between thus obtained sedimentation coefficients between the c(s) and ls-g*(s) model is as well apparent (Fig. 2d). The corresponding concentration dependences of the average sedimentation coefficients are shown in Fig. 2b and d. We see that in case of CMC 1 all sedimentation coefficients can be approximated by a single linear fit, while the sedimentation coefficients for CMC 10 reveal different dependences depending on the degree of dilution. For example, in the concentrated regime $1.7 \leq c[\eta] \leq 5.1$ (filled squares in Fig. 2d), we would obtain a sedimentation coefficient at infinite dilution of $s_0 = 2.77\,S$, while for the semi-dilute solutions with $0.8 \leq c[\eta] \leq 1.7$ (half-filled squares in Fig. 2d), we would obtain a value of $s_0 = 3.34\,S$, and for the dilute regime with $0.2 \leq c[\eta] \leq 0.4$ (empty squares in Fig. 2d) a value of $s_0 = 5.07\,S$. Clearly, this resembles a very large range of s_0 values. Thus, only the dilute regime (empty squares in Fig. 2d) appears to be suitable for extrapolation to infinite dilution. The concentration dependences of s^{-1} according to Eq. (S4) for all studied CMC samples from the $c(s)$ model are shown in Fig. S7. Based on the approximate linear description of the concentration dependence of the sedimentation coefficient (Eq. (S4)), we can consider the ratio s_0/s as a function of dilution, $c[\eta]$ (Eq. (4)). Fig. 3 displays this global plot including all CMCs for $c[\eta] < 6$ toward the experimentally smallest possible concentration. The experimental data clearly reveals that there is a transition from the dilute regime over the semi-dilute toward the concentrated regime of s_0/s on $c[\eta]$ (Eq. (4)).

At very high degrees of dilution $c[\eta] < 0.1$, a practical approximation of s_0 even without any extrapolation becomes possible with an error of $\leq 10\,\%$ only, while this error reduces to less than $\leq 5\,\%$ at even

higher dilution, $c[\eta] < 0.05$. At further increases in $c[\eta]$, beyond that shown in Fig. 3 the dependence may reach a plateau again (Fessler & Ogston, 1951; Mijnlieff & Jaspers, 1971; Pavlov & Frenkel, 1983). At such high $c[\eta]$ values, the macromolecular structures overlap with a more or less defined homogeneous distribution of the macromolecular segments of individual macromolecules throughout the available solution volume. In this instance, the sedimentation process in the centrifuge cell can in turn be considered as (directionally opposite) solvent flow through a macromolecular mesh and not the movement of individual macromolecules through solvent. Under several assumptions, an interrelation between the actual sedimentation coefficient and an effective medium permeability can be established (Mijnlieff & Jaspers, 1971).

Plots such as in Fig. 3 as well provide guidance for a suitable degree of dilution, $c[\eta]$ (Eq. (4)), to be considered for the sedimentation velocity experiments and respective data evaluation, in order to receive the most accurate values of the sedimentation coefficients at infinite dilution, or being practically close to the value at infinite dilution.

The slope of the concentration dependence of sedimentation coefficients over appropriate ranges of concentration can be used to calculate the Gralen coefficient, k_s (the concentration-sedimentation coefficient). The k_s values can be considered as a "translational friction" analogue of the intrinsic viscosity, $[\eta]$, having the same physical units of cm^3g^{-1} and expressed as:

$$k_s = B\frac{<h^2>^{3/2}}{M} \tag{5}$$

where B in units mol^{-1} is a parameter that depends on the relative contour length, L/A, and relative diameter of macromolecular chains, d/A (Pavlov, 1996).

The dimensionless ratio $k_s/[\eta]$ (the Wales-van-Holde ratio) can then be used as a characteristic for different macromolecule conformations (vide infra) (Harding, 1995; Wales & Van Holde, 1954). Additionally, the conformational state of the macromolecules may directly be assessed through plotting the Gralen coefficients, k_s, against the sedimentation coefficients at infinite dilution, s_0, on a double logarithmic scale (Fig. S8), without the necessity of knowledge of the actual molar mass values of the CMC samples. Such plot ($k_s = Ks_0^{b_{ks s0}}$) represents an analogue of the classical scaling relationships of Kuhn-Mark-Houwink-Sakurada (KMHS) between the hydrodynamic characteristics and the molar mass (vide infra). Using the estimated scaling index, $b_{ks s0}$, one can estimate the scaling index b_{s0} in the corresponding KMHS relationship, $s_0 = KM^{b_{s0}}$, by the basic relation $b_{s0} = 2/(b_{ks s0} + 3)$. The experimentally evaluated value of $b_{ks s0} = 1.69 \pm 0.07$ results in a value of $b_{s0} = 0.43$. The value of $b_{s0} = 0.43$ is slightly larger than the literature data for the CMC macromolecules (Lavrenko et al., 1999; Sitaramaiah & Goring, 1962). A more detailed discussion and comparison of the b_{s0} from the $b_{ks s0}$ to the independently determined values of b_{s0} will be provided later. The accuracy of such evaluations will depend on many factors, such as the range of the studied molar masses, the dispersity and heterogeneity of the macromolecules, the macromolecule-solvent interactions, and the reliability of the experimental data.

3.4. Translational friction II – diffusion

Diffusion coefficients are inherently difficult to determine in an absolute manner. The perhaps most popular method is based on dynamic light scattering (DLS). In case of the CMCs studied, the adequate analysis by batch DLS provided hurdles, because of their high dispersity / heterogeneity. Another opportunity to determine diffusion coefficients is the use of sedimentation velocity data via a direct Lamm equation modeling (Eq. (S3)).

The $c(s)$ and $c(s, f/f_0)$ analysis is based on the numerical solution of the Lamm equation, returning f/f_{sph} values, that are, together with the sedimentation coefficient and partial specific volume, characteristic of diffusion coefficients, D, at a given solution concentration, respectively at infinite dilution, D_0 (Schuck, 2000):

$$D_0 = \frac{k_B T(1-\upsilon\rho)^{1/2}}{\eta_0^{3/2} 9\pi\sqrt{2}((f/f_{sph})_0)^{3/2}(s_0\upsilon)^{1/2}} \tag{6}$$

This equation allows estimation of the diffusion coefficient at infinite dilution, D_0, through the hydrodynamic equivalent sphere concept. This opportunity was demonstrated to result in adequate values for synthetic macromolecules of a random coil conformation and a narrow unimodal molar mass distribution (Grube et al., 2018; Nischang et al., 2017), and was initially attempted for the here investigated samples.

Fig. S9 shows a comparison of the estimated f/f_{sph} values, by both the $c(s)$ and the $c(s, f/f_0)$ model for the CMC 1 and CMC 10 examples. On first sight, both models, in general, provide frictional ratios, f/f_{sph}, closer to each other at larger macromolecule solution concentrations and more different at lower macromolecule solution concentrations.

The CMC 1 sample shows a nonlinear concentration dependence of f/f_{sph} values (Fig. S9a), yet the corresponding dependence of the weight (signal) average sedimentation coefficients, s, was approximately linear over the same range of concentrations (Fig. 2b). The frictional ratios at infinite dilution are $(f/f_{sph})_0 = 2.3$ for the $c(s)$ and $(f/f_{sph})_0 = 3.1$ for the $c(s, f/f_0)$ model, correspondingly. Though appearing to be in a physical range, these values differ significantly, providing doubt for their correctness as discussed in the next section.

While apparent frictional ratios, $f/f_{sph} > 30$, are received from modeling sedimentation velocity data for the CMC 10 (Fig. S9b), similar based on both models (the $c(s)$ and $c(s, f/f_0)$) under concentrated macromolecule solution conditions, in dilute solutions, the frictional ratios, f/f_{sph}, follow very strong linear concentration dependence resulting in $(f/f_{sph})_0 \approx 0$ for the $c(s)$, and $(f/f_{sph})_0 = 5.2$ for the $c(s, f/f_0)$ models, correspondingly. The estimation by the $c(s)$ model appears simply unphysical, since CMC macromolecules in solutions would provide lower frictional ratios, f/f_{sph}, than a spherical particle of the same anhydrous volume and mass, while the value evaluated by the $c(s, f/f_0)$ model appears more realistic on first sight. Irrespective these aspects, the root mean square deviation ($rmsd$) values from modelling sedimentation data seemed acceptable, e.g. $rmsd = 0.0042$ fringes for CMC 1 at a concentration of $c = 3x\,10^{-3} g\,cm^{-3}$ and $rmsd = 0.0072$ fringes for CMC 10 at a concentration of $c = 2.44x\,10^{-3} g\,cm^{-3}$ for the $c(s)$ model.

Clearly, boundary anomalies as well as dispersity and heterogeneity of the macromolecular samples make the correct estimation of frictional properties very difficult by numerical approaches currently available. These problems very likely originate from the boundary sharpening and Johnston-Ogston effect at to be studied high concentrations, respectively, the very pronounced dispersity / heterogeneity of the samples manifested at lower concentrations (Figs. S6 and 2) (Chaturvedi et al., 2018; Fujita, 1956; Johnston & Ogston, 1946). This situation contrasts that found for ideally behaving macromolecules of narrow dispersity (Grube et al., 2018; Nischang et al., 2017), respectively proteins (Schuck, 2000), studied at appropriate degrees of dilution.

Independently, the values of the diffusion coefficients, D, were determined by the solvent-solution boundary experiments in the centrifuge. Unfortunately, with the present experimentally possible implementation using refractive index detection, the lowest possible concentration to study was $c \approx 1 \times 10^{-3} g\,cm^{-3}$; below this value the signal-to-noise ratio was too small to adequately analyze the experimental data over large enough boundary spreading times. However, the evaluation of sedimentation coefficients, s, considering statistical random noise through numerical modeling of the Lamm equation provided no roadblock. Corresponding example plots of the boundary dispersion, σ^2, against time, t, are shown in Fig. S10. Concentration dependences of the calculated diffusion coefficients, D, are displayed in Fig. S11 and the data is summarized in Table 1 (vide infra). Importantly, the high molar mass samples had to be studied in

Table 1
Intrinsic viscosities, $[\eta]$, sedimentation coefficients at infinite dilution, s_0, diffusion coefficients at infinite dilution, D_0, hydrodynamic invariants, A_0 (Eq. (7)), and the sedimentation parameters, β_s (Eq. (8)), for all CMCs in 0.1 M aqueous sodium chloride at $T = 20.0\,°C$.

Sample	$[\eta]$ cm^3g^{-1}	s_0 S	D_0 $10^{-7}\,cm^2s^{-1}$	A_0 $10^{-10}\,g\,cm^2\,s^{-2}K^{-1}\,mol^{-1/3}$	β_s $10^7\,mol^{-1/3}$	$k_s/[\eta]$
CMC 1	173	1.86	2.26	3.31	1.28	1.53
CMC 2	228	2.08	1.98	3.44	1.25	1.25
CMC 3	676	3.18	1.07	3.78	1.23	0.91
CMC 4	535	2.67	1.20	3.56	1.16	0.91
CMC 5	609	2.83	0.97	3.29	1.11	1.01
CMC 6	642	3.02	0.97	3.42	1.11	0.90
CMC 7	596	3.46	0.95	3.45	1.24	1.22
CMC 8	1193	4.43	0.44	(2.82)	(0.95)	1.01
CMC 9	1347	5.36	0.35	(2.69)	(0.92)	1.06
CMC 10	1710	5.07	0.45	3.38	1.08	0.87

concentrated solutions in instances ($c[\eta]$, Eq. (4)), such that solution non-ideality could impose some bias. Possible experimental inconsistencies are discussed in the next section.

3.5. Consistency of the experimental data from rotational and translational friction

To this end, we have discussed the evaluation of the primary hydrodynamic characteristics, i.e. intrinsic viscosities, $[\eta]$, sedimentation coefficients at infinite dilution, s_0, with corresponding Gralen coefficients, k_s, and attempts to determine frictional ratios, $(f/f_{sph})_0$, respectively, diffusion coefficients, D_0, at infinite dilution. As mentioned above, these hydrodynamic characteristics are related to the same macromolecular characteristics – the molar mass and the hydrodynamic volume / size that may be expressed via the macromolecules chain end-to-end distance, $<h^2>$, (Eqs. (1–3) and (5)). The relationship between these macromolecular characteristics can be established via the hydrodynamic invariant, A_0, (Eq. (7)) (Tsvetkov, Lavrenko, & Bushin, 1984) or sedimentation parameter, β_s, (Eq. (8)) (Pavlov, 1996; Pavlov et al., 2011):

$$A_0 = (R[s][D]^2[\eta])^{1/3} = (\mathrm{M}[\eta])^{1/3}[D] = R[s][\eta]^{1/3}M^{-2/3} \quad (7)$$

$$\beta_s = k_B^{-2/3}(N_A[s][D]^2k_s)^{1/3} = (Mk_s)^{1/3}[D]k_B^{-1} = N_A[s]k_s^{1/3}M^{-2/3} \quad (8)$$

where $[s] = s_0\eta_0/(1 - \upsilon\varrho_0)$ is the intrinsic sedimentation coefficient, and $[D] = D_0\eta_0/T$ is the intrinsic diffusion coeffcient. Eqs. (7) and (8) as well highlight the relatively high importance of adequate values of the intrinsic diffusion coefficients, $[D]$, due to their higher exponential power.

In the literature, distinct characteristic values of A_0 (Eq. (7)) and β_s (Eq. (8)), established for all basic macromolecular systems in solution are available. The concept of A_0 enables verification of the hydrodynamic data – low fluctuations around the average values known for a particular type of macromolecules allow to state that a consistent correlation between different hydrodynamic characteristics is achieved. Though there are no sharp boundaries between the reported literature values, there are upper and lower limiting values for A_0 (Tsvetkov et al., 1984), also listed in Table S3.

Values of the hydrodynamic invariants, A_0, the sedimentation parameters, β_s, and the Wales-van-Holde ratio, $k_s/[\eta]$, show an agreement with the reported literature data for CMCs (Table 1) (Lavrenko et al., 1991, 1999; Tsvetkov, 1989; Tsvetkov et al., 1984). Attention, however, should be payed to some high molar mass samples (e.g. CMCs 8 and 9), where the values of the invariants, A_0, are below or close to the theoretical minimum limit of $A_0 = 2.9x\,10^{-10}g\,cm^2\,s^{-2}K^{-1}\,mol^{-1/3}$ for a solid impermeable sphere (Tsvetkov et al., 1984), and diverge from the other studied samples. Interestingly, these samples also feature the smallest sedimentation parameters, β_s.

The obstacles can be traced back to non-adequate values of the diffusion coefficients, D_0, since the studied concentration range corresponds, in this case, to concentrated solutions ($c[\eta]$, Eq. (4)). Furthermore, considering the values of the diffusion coefficients calculated from the frictional ratios obtained from the $c(s)$ and $c(s, f/f_0)$ models (Eq. (6)), correspondingly, leads to $A_0 = 6.4x\,10^{-10}g\,cm^2\,s^{-2}\,K^{-1}\,mol^{-1/3}$ and $A_0 = 4.7x\,10^{-10}\,g\,cm^2\,s^{-2}K^{-1}\,mol^{-1/3}$ for the CMC 1. Such estimations appear larger than macromolecule systems reported in the literature, also as the upper theoretical limit so far (Tsvetkov et al., 1984). It clearly indicates that, in this case, the diffusion coefficients, D_0, are again incorrectly estimated. A similar situation was found for the high molar mass sample (CMC 10) using the data from the $c(s, f/f_0)$ model; the value of the intrinsic diffusion coefficients $[D]_{(f/f_{sph})_0} = 3.68x\,10^{-12}g\,cm\,s^{-2}\,K^{-1}$ is giving a value of $A_0 = 6.0x\,10^{-10}\,g\,cm^2\,s^{-2}\,K^{-1}\,mol^{-1/3}$. Once more, this details that in contrast to ideal macromolecule populations of a random coil conformation and a narrow unimodal dispersity, the hydrodynamic equivalent sphere concept (Eq. (6)) has very limited suitability for the here studied samples to properly resolve diffusion by numerical solution of the Lamm equation (Eq. (S3)). Fortunately, with this information at hand we can track and address this obstacle by average hydrodynamic parameters obtained for other CMC samples in the present study (vide infra).

3.6. Size exclusion chromatography-multi-angle laser light scattering (SEC-MALLS)

Normalized refractive index and MALLS@90°elugrams for CMCs 1 and 10 are shown in Fig. 4a and b. It is clearly observable that concentration-sensitive refractive index detection and mass-sensitive MALLS detection resemble different detector profiles. However, both are used for molar mass estimations via light scattering (Grube et al., 2018). Example Zimm plots can be seen in Fig. S12. M_i values were estimated in elution regions were both detectors showed a sufficient signal-to-noise ratio (Fig. 4). In any case, for determination of the $M_w = M_{SEC-MALLS}$ estimates of the populations of macromolecules, the appropriate elution fractions, utilizing refractive index and MALLS data of individual elution slices, were considered. All individual traces are shown in Fig. S13 for each of the remaining CMCs 2–9, while a comparison of all refractive index-elution traces can be found in Fig. S14.

3.7. Molar mass determinations

In the present case of CMCs, i.e. highly disperse, charged, and non-ideal systems, the main aim is the estimation of statistically most relevant values of the molar mass that describe this highly disperse set of macromolecules most comprehensively, particularly in concert to all determined average macromolecular characteristics. Having established values of the sedimentation coefficients at infinite dilution, s_0, diffusion coefficients at infinite dilution, D_0, and the partial specific volume, υ, enables calculation of the molar masses by the classical Svedberg relationship, $M_{s,D}$:

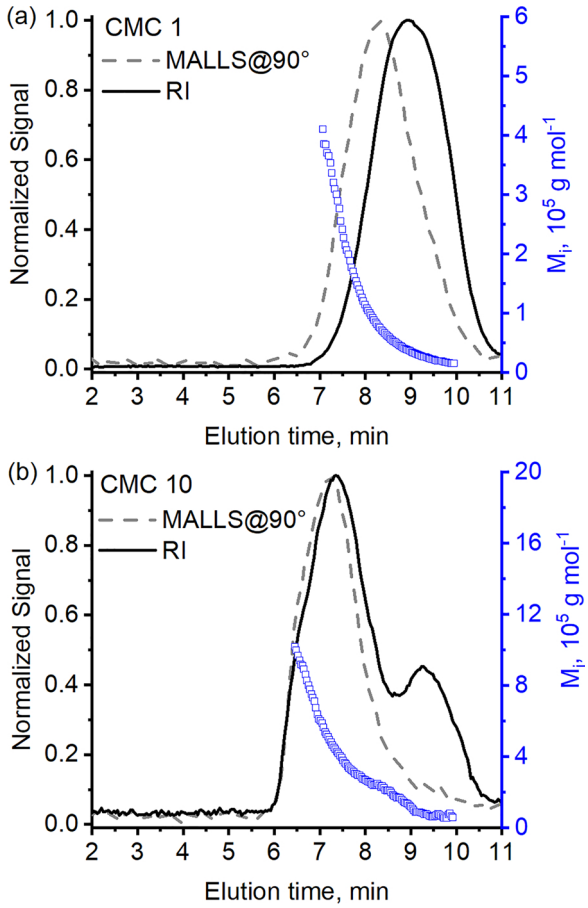

Fig. 4. Normalized SEC refractive index (solid black lines) and MALLS@90° (dashed gray lines) elution profiles in 0.1 M aqueous sodium chloride at $T = 25.0\,°C$ for (a) CMC 1 and (b) CMC 10, together with the respective molar mass traces, M_i (empty blue squares), in elution regions with sufficient signal-to-noise ratio. (For interpretation of the references to colour in this figure legend, the reader is referred to the web version of this article).

$$M_{s,D} = \frac{s_0 RT}{D_0(1 - \upsilon\varrho_0)} = R\frac{[s]}{[D]} \tag{9}$$

The molar masses calculated, $M_{s,D}$, (Eq. (9)) are compared to the values evaluated by SEC-MALLS ($M_{SEC-MALLS}$) via the concept of the hydrodynamic invariant, A_0 (Eq. (7)) assuming known gross average values (Table S3) (Tsvetkov et al., 1984). In Fig. 5 we see that, in general, some correlation between the $M_{s,D}$ and $M_{SEC-MALLS}$ values is obtained.

Since the hydrodynamic invariant is based on three different basic characteristics (Eq. (7)), its value should be allowed to fluctuate around its means while upper theoretical limits and the lower, represented by a solid impermeable sphere, were chosen as boundaries for allowance of such fluctuations (Fig. 5).

For CMC samples 1–10 the sedimentation coefficients, s_0, were evaluated from the concentration dependences within the highly dilute to semi-dilute regions ($c[\eta]$, Eq. (4)). However, the diffusion coefficients, D_0, had to be determined from the semi-dilute to concentrated solutions, particularly in cases of CMCs 8-10. Thereby, some of the high molar mass samples investigated by analytical ultracentrifugation (CMCs 8 and 9) show A_0 values below, or close to, the theoretical limit, since the diffusion coefficients are incorrectly estimated. In analogy, an underestimation of the k_s value in case of concentrated solutions would as well decrease the value of the sedimentation parameter, β_s (Figs. 2 and S7).

In such cases, the statistically most suitable molar masses of the

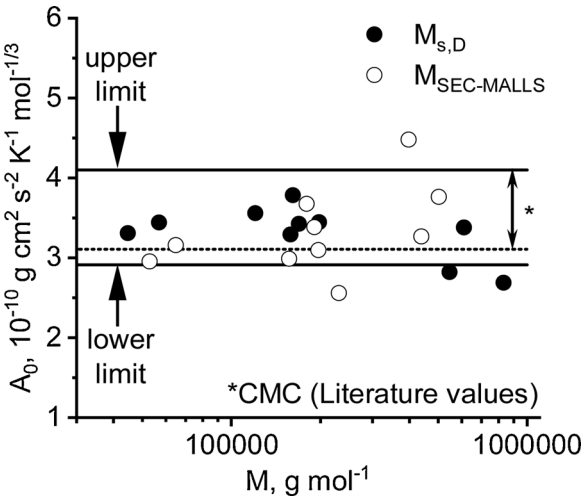

Fig. 5. Comparison of the hydrodynamic invariants, A_0 (Eq. (7)), calculated using molar masses determined by sedimentation-diffusion analysis, $M_{s,D}$, and light scattering, $M_{SEC-MALLS}$. Upper and lower limits according to Tsvetkov et al., 1984.

respective populations can be calculated based on the average determined values of the hydrodynamic invariant, A_0 (Eq. (7)), or sedimentation parameter, β_s (Eq. (8)). The following relationships, where diffusion is substituted by the hydrodynamic invariant, A_0 (Eq. (10)), respectively, the sedimentation parameter, β_s (Eq. (11)) were used:

$$M_{s,\eta} = \left(\frac{R}{A_0}\right)^{3/2} ([s]^3[\eta])^{1/2} \tag{10}$$

$$M_{k,s} = (N_A[s]/\beta_s)^{3/2} k_s^{1/2} \tag{11}$$

In analogy, the diffusion coefficients, D_0, could be calculated by Eqs. (7) and (8) with a proper mathematical re-arrangement. The average values of the physically-sound invariants (Table 1) used from the present study were $A_0 = (3.45 \pm 0.16)\,x\,10^{-10} g\,cm^2\,s^{-2}\,K^{-1}\,mol^{-1/3}$ and of the sedimentation parameter, $\beta_s = (1.18 \pm 0.08)\,x\,10^7\,mol^{-1/3}$. These are in excellent agreement with the established average values of the invariants of related (cellulose) macromolecules from other reports (Pavlov, 1996; Tsvetkov et al., 1984) and do represent a physically-sound range of values known from the literature (Fig. 5, Table S3).

The SEC-MALLS analysis in general shows higher fluctuations over A_0 values (Fig. 5). At least two samples reveal values clearly out of to be considered range (CMCs 5 and 10). The overall values of the molar masses are summarized in Table 2. Interestingly, CMCs 1–6 feature higher molar masses when investigated with SEC-MALLS, $M_{SEC-MALLS}$, as compared with sedimentation-diffusion, $M_{s,D}$, values. In our further

Table 2
Molar masses evaluated by sedimentation-diffusion analysis, $M_{s,D}$, SEC-MALLS, $M_{SEC-MALLS}$, calculated by the invariant, $M_{s,\eta}$ (eq. 10), and the sedimentation parameter, $M_{k,s}$ (eq. 11).

Sample	$M_{s,D}$ g mol^{-1}	$M_{SEC-MALLS}$ g mol^{-1}	$M_{s,\eta}$ g mol^{-1}	$M_{k,s}$ g mol^{-1}	M_{av} g mol^{-1}
CMC 1	45,000	53,000			49,000
CMC 2	57,000	65,000			61,000
CMC 3	162,000	191,000			177,000
CMC 4	121,000	157,000			139,000
CMC 5	158,000	(231,000)	148,000	144,000	150,000
CMC 6	169,000	197,000			183,000
CMC 7	198,000	180,000			189,000
CMC 8	(547,000)	439,000	405,000	396,000	413,000
CMC 9	(832,000)	503,000	573,000	574,000	550,000
CMC 10	612,000	(397,000)	593,000	538,000	581,000

discussion, we will operate with the average values, M_{av}, between $M_{s,D}$, $M_{SEC-MALLS}$, as well as the invariant and sedimentation parameter molar masses, $M_{s,\eta}$, and $M_{k,s}$ (see Table 2).

The samples characterized by A_0 values outside of the theoretical limits were excluded from the averaging, i.e. CMCs 8 and 9 for hydrodynamic analysis and CMCs 5 and 10 for SEC-MALLS analysis. In that way, we seek a maximum of statistical reality reflected by the experiments, and eliminate an ill-founded absolute result of molar mass estimation in clearly identified cases.

3.8. Approaches to access conformation in solution

3.8.1. Classical scaling relationships

Having statistically adequate values of the molar masses from a multiplicity of orthogonal experiments, M_{av}, (Table 2) at hand, we can now move to the conformation of the CMC macromolecules in solution using the classical scaling relationships known also as Kuhn-Mark-Houwink-Sakurada (KMHS) relationships. Most frequently, these relationships are represented by the scaling of the intrinsic viscosity, $[\eta]$, versus the molar mass, M:

$$[\eta] = K_{[\eta]} M^{b_{[\eta]}} \tag{12}$$

Similar relationships can be established for each pair of the hydrodynamic characteristics and the molar mass, M:

$$s_0 = K_{s_0} M^{b_{s_0}} \tag{13}$$

$$D_0 = K_{D_0} M^{b_{D_0}} \tag{14}$$

The corresponding double logarithmic dependences by using average values of the molar mass, M_{av}, are shown in Fig. 6. Note, that for CMCs 8 and 9 the diffusion coefficients, D_0, were calculated using average values of the invariants by re-arrangement of Eqs. (7) and (8). The magnitude of the scaling indices are typical for CMC and cellulose derivatives in general. (Arinaitwe & Pawlik, 2014; Eremeeva & Bykova, 1998; Lavrenko, Okatova, Tsvetkov, Dautzenberg, & Philipp, 1990, 1991; Lavrenko et al., 1999)

The interrelation between different scaling indexes ($|b_{D_0}| + b_{s_0} = 1$ and $|b_{D_0}| = (1 + b_{[\eta]})/3$) is within the experimental error. Furthermore, the previously estimated b_{s_0} value from the k_s over s dependence with $b_{s_0} = 0.43$ practically coincides with the $b_{s_0} = 0.42 \pm 0.02$ value determined from the classical s_0 over M dependence. Knowledge of the adequacy of absolute values of the diffusion coefficients, D_0, determined by synthetic boundary experiments and / or from the hydrodynamic invariant (Eq. (7)) allows for the calculation of frictional ratios, $(f/f_{sph})_0$, known from the definition of the diffusion coefficient by the hydrodynamic equivalent sphere concept and accessible by re-arrangement of Eq. (6). As shown in the Supporting Information (Fig. S15), the apparent $(f/f_{sph})_0$ estimates assume values of $4 < (f/f_{sph})_0 < 10$, underpinning that the CMCs in the present study are far away from being comparable to the spherical approximates, further amplified by the dispersity and heterogeneity of the present samples, strongly manifested at high degrees of dilution, $c[\eta]$ (Eq. (4)) (Figs. 2 and S6). Again, this makes sedimentation-diffusion analysis by numerical solution of the Lamm equation a currently impossible endeavor. As seen in Fig. S15 a double logarithmic scaling of the calculated frictional ratios shows a slope of $b_{(f/fsph)_0} = 0.28$ fulfilling the basic relation $b_{(f/fsph)_0} + 1/3 = b_{D_0}$ (Fig. 6). This situation further underpins the power of the here presented fundamental model-free hydrodynamic experimental approaches for non-ideal systems. The above-mentioned issues and their explanation are also a fundamental testament of the situation that once adequate values of the hydrodynamic invariants are established, the interrelation of scaling relationships should be fulfilled as well, a situation re-affirmed in the present study as well as in our previous work (Grube et al., 2018; Nischang et al., 2017).

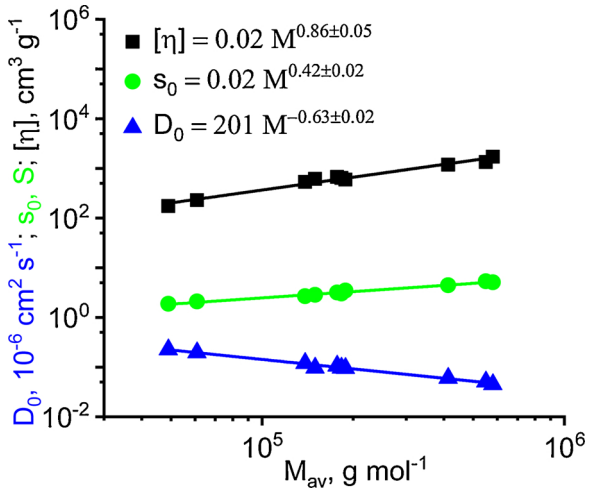

Fig. 6. Double logarithmic scaling relationships of $[\eta]$, s_0, and D_0 against average values of the molar mass, M_{av}, for the CMC samples in 0.1 M aqueous sodium chloride at a temperature of $T = 20.0\,°C$. (For interpretation of the references to colour in this figure legend, the reader is referred to the web version of this article).

The knowledge of the scaling relationship for sedimentation allows for calculation of the dispersity of CMCs via the Fujita approach (Fujita, Hutchinson, & Van Rysselberghe, 2016) as exemplified for CMCs 1 and 10 in the Supporting Information using the here established scaling relationship of sedimentation (Fig. 6). Therefore, transformation of the differential distribution of sedimentation coefficients ($c(s) = dc/ds$) to a differential distribution of molar masses (dc/dM) was pursued (Fig. S16). In fact, also the dispersity, $Đ$, as the ratio of the weight- and number-average molar mass, $Đ = M_w/M_n$ depends on the degree of dilution, $c[\eta]$ (Eq. (4)), reaching values for the CMC 1 and CMC 10 of $Đ > 10$, while apparently low dispersities of close to one are observed under self-sharpening conditions and the Johnston-Ogston effect (vide supra, Figs. 2 and S6).

3.8.2. Kuhn segment length and macromolecular chain parameters

The conformation of macromolecular chains can be described by the corresponding structural chain parameters. The Kuhn segment length, A, or persistence length ($a = A/2$), along with the diameter of the macromolecule chain, d, determines its conformation and solution behavior. The flexibility and corresponding conformation will primarily depend on the chemical structure of the macromolecules and their interactions with the solvent. The choice of the appropriate theory describing the behavior of macromolecular chains for the estimation of the conformational parameters can be put forward based on the evaluated values of the scaling indices. In reference to the literature, there are certain ranges of values of scaling exponents for gauging conformation of macromolecules, i.e. for intrinsic viscosity, for sedimentation, or for diffusion. In example, $b_{[\eta]} = 1.8$, $b_s = 0.15$, $b_D = 0.85$, for a rigid rod, and $b_{[\eta]} = 0.5 - 0.8$, $b_s = 0.4 - 0.5$, $b_D = 0.5 - 0.6$ for random coils (Harding, 1995).

In general, if $b_{[\eta]} > 0.8$ or $b_s < 0.4$ (rigid chain-macromolecules), the analysis of the experimental data should be performed considering the theories accounting for intra-chain draining effects only. When $b_{[\eta]} < 0.8$ or $b_s > 0.4$ (flexible chain macromolecules) the corresponding estimations of the conformational parameters should be performed considering only the excluded volume effects, i.e. neglecting the intra-chain draining effects (Pavlov et al., 2011).

In our case of $b_{[\eta]} = 0.86$ and $b_s = 0.42$, the major issue is to make a suitable choice between the draining and excluded volume effects, respectively take both of them into account. Cellulose and its (ionic) derivatives are known as semi-rigid / semi-flexible polymer chains, and therefore, one should expect a much lower influence of the excluded volume effects compared to flexible macromolecular chains. This is because, the much lower degree of coiling for the rigid / semi-rigid

macromolecular chains should naturally decrease the possibility of long ranged contacts between chain elements. The deviations from the Gaussian statistics, experimentally observed for various cellulose derivatives in solutions, were interpreted by their high structural rigidity (Schulz & Penzel, 1968; Tsvetkov, 1989). Notwithstanding, the here observed scaling indices may make the suitable choice of the respective model for analysis of chain-conformational characteristics less straightforward (vide supra).

In a series of papers, Lavrenko and coauthors (Lavrenko et al., 1990, 1991; Lavrenko, Okatova, Dautzenberg, & Philipp, 1993, 1999; Okatova, Lavrenko, & Dautzenberg, 2000), reported the hydrodynamic analysis of different CMC fractions in water / cadoxen mixtures by using the Yamakawa-Fujii theory for the wormlike cylinder model and by considering the absence of the excluded volume effects (Yamakawa and Fujii, 1973). However, there are studies which do consider the excluded volume effects in the estimations of the conformational parameters of cellulose and its derivatives (Davis, 1991; Kamide, Saito, & Suzuki, 1983). One of the most advanced theories describing translational friction is the Gray-Bloomfield-Hearst (GBH) theory that is based on the worm-like necklace model (Gray, Bloomfield, & Hearst, 1967):

$$[s]P_0N_A = \frac{3M_L^{\frac{1+\varepsilon}{2}}M^{\frac{1-\varepsilon}{2}}}{(1-\varepsilon)(3-\varepsilon)A^{\frac{1-\varepsilon}{2}}} + \left(\frac{P_0M_L}{3\pi}\right)\left(\frac{\ln A}{d} - \varphi(\varepsilon)\right) \quad (15)$$

where $\varphi(\varepsilon) = 1.431 + 2.64\varepsilon + 4.71\varepsilon^2$, $M_L = M_0/\lambda$, $M_0 = 162.1 + 81\,DS$, $\lambda = 5.15\,x\,10^{-8}\,cm$, and $P_0 = 5.11$ being Flory's hydrodynamic parameter. M is the molar mass of the macromolecule chain, M_0 is the mass of the monomer unit calculated from values of the degree of substitution, DS, of the CMCs (Table S1), and λ is the projection of the monomer unit toward the fully extended macromolecule chain. The value of $\lambda = 5.15\,x\,10^{-8}\,cm$ reported for cellulose and its derivatives was used (Pavlov, 1996).

The excluded volume effects are characterized by the thermodynamic parameter ε, which can be calculated based on the determined values of the scaling indices ($\varepsilon = 1 - 2b_s = 2\,|b_D| - 1 = (2b_\eta - 1)/3$). In case of absence of the excluded volume effects ($\varepsilon = 0$) the GBH theory (Eq. (15)) transforms into the corresponding theory of Yamakawa-Fujii with $\varphi(0) = 1.056$. Fig. 7 shows corresponding dependences of $[s]P_0N_A$ on the $M^{\frac{1-\varepsilon}{2}}$ in cases of ε being $\varepsilon = 0.20$ representative of the excluded volume effects, and $\varepsilon = 0$, representative of their absence.

The Yamakawa-Fujii theory gives values of $A = 25 \pm 1\,nm$ and $d = 1.6 \pm 0.5\,nm$. The GBH theory gives $A = 14 \pm 1\,nm$ and $d = 2 \pm 2\,nm$. The first estimate of A is in good agreement with the reported literature data on CMC samples mentioned above, however showing slightly higher values. This can be explained by the contribution of short-ranged electrostatic interactions that may even remain at the here utilized sodium chloride concentration in solution.

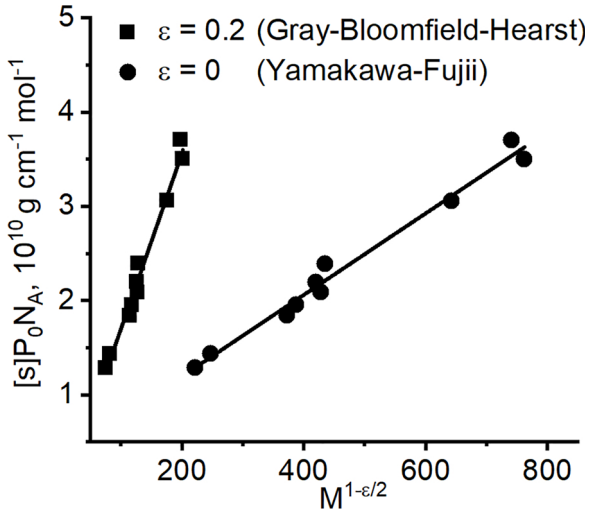

Fig. 7. Kuhn segment length estimations using the Gray-Bloomfield-Hearst (GBH) and Yamakawa-Fujii theory for the CMC samples in 0.1 M aqueous sodium chloride at a temperature of $T = 20.0\,°C$.

In case of the GBH theory we arrived at notably lower values of A, which in this case can be associated with the possible overestimation of the excluded volume effects by the use of the parameter ε, based on the here determined scaling relationships. This is associated to the yet unknown contributions from the intra-chain draining and excluded volume effects and their interplay, which cannot be described with current theories at hand. Therefore, a final analysis remains elusive.

3.8.3. Conformation zone plots

Another elegant, less close to tedious experiment, approach to estimate conformation of macromolecules in solution was reported by Pavlov, Rowe, & Harding (1997). Here, a double logarithmic plot of the product of the Gralen coefficient (Eqs. (5) and (S4)) and mass per unit length of the macromolecule, k_sM_L, against the ratio of intrinsic sedimentation coefficient and mass per unit length of the macromolecule, $[s]/M_L$, is used. The product $k_sM_L \sim <h^2>^{3/2}/L \sim V/L$, i.e. the volume occupied per contour length of the macromolecule. The ratio $[s]/M_L \sim L/<h^2>^{1/2}$ is characteristic of the macromolecular degree of coiling, i.e. the contour length per chain end-to-end distance of the macromolecules.

Macromolecules having different conformational properties occupy different zones in a double logarithmic graphical representation of k_sM_L against $[s]/M_L$, such as displayed in Fig. 8. The drawn boundaries should be considered approximate only, since there is no sharp transition from zone to zone, a similar situation faced with the hydrodynamic invariant (vide supra). While our present data are highlighted in blue, we also show available data from the literature on CMCs as well as structurally related methylcellulose and cellulose nitrate.

Our data, as well as literature data, are located within the semi-flexible / semi-rigid conformation zone, a result in agreement with the above presented analysis by the scaling relationships as well as excellent agreement with the molecular chain properties. There is clear

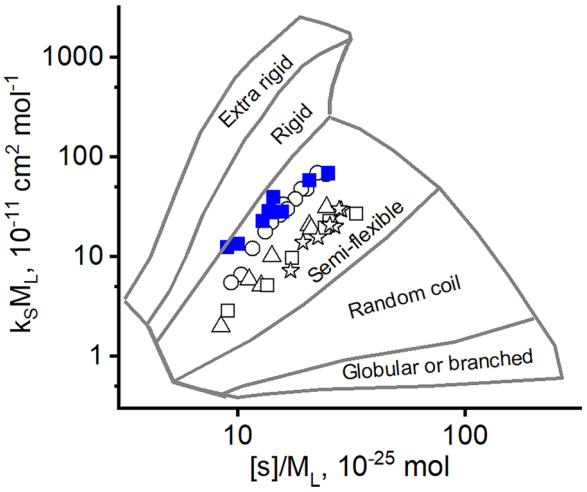

Fig. 8. Conformation zone plots to indicate conformational properties of the CMCs 1 to 10 in 0.1 M aqueous sodium chloride at a temperature of $T = 20.0\,°C$ (filled blue squares). Shown also are data from Pavlov et al. on polysaccharides (empty black squares) (Pavlov, 1996), from Pavlov et al. on cellulose nitrate (empty black circles) (Pavlov & Frenkel, 1983), CMCs investigated in cadoxen / water mixtures from Lavrenko et al. (empty black triangles) (Lavrenko et al., 1991), and CMCs investigated in cadoxen / water from Lavrenko et al. (empty black stars) (Lavrenko et al., 1999). (For interpretation of the references to colour in this figure legend, the reader is referred to the web version of this article).

indication, that the conformation of the CMCs is characterized by significant backbone rigidity compared to the literature examples, partly due to residual backbone charge effects. Such conformation zoning bears potential to determine structural properties of macromolecules with very limited experimental effort based on sedimentation velocity experiments at appropriate degrees of dilution, $c[\eta]$ (Eq. (4)), (Fig. 3). Also such conformation zoning can represent an excellent complement to the classical scaling relationships and statistical chain characteristics in solution (vide supra).

4. Conclusions

We have demonstrated and explained how readily disperse, charged, and unfractionated macromolecule populations can quantitatively be studied by the methods of molecular hydrodynamics and light scattering, exemplified with one of the derivatives of the most abundant natural macromolecules of very high dispersity / heterogeneity at hand, i.e. sodium carboxymethyl cellulose (CMC). Particular success for such study is the combination of several orthogonal analytical techniques that, despite their different insights, can bring physical consistency to the behavior of macromolecules in solution.

Our study highlights as well the very limited insight provided by a single analytical technique used for characterization of a given sample of macromolecules at hand, e.g. an estimated molar mass from light scattering only. This is approached by studying intrinsic viscosities, (intrinsic) sedimentation coefficients, and (intrinsic) diffusion coefficients that all describe macromolecular systems in solution with a different, though highly orthogonal, perspective.

Interestingly, data from sedimentation velocity analysis in the ultracentrifuge (Figs. 2 and S6) and size exclusion chromatography coupled to multi-angle laser light scattering (Figs. 4 and S13), highlight the comparable insight on dispersity and heterogeneity of the samples. The strongly manifested dispersity / heterogeneity of the macromolecule populations at high degrees of dilution makes the use of sedimentation-diffusion analysis in terms of direct modeling of the Lamm equation difficult, the highly concentrated regime leads to unusually large frictional ratios due to boundary sharpening (Figs. S6 and S9). In identified cases, boundary shape is not solely determined by diffusion, but by the widely varying sedimentation coefficients originating from high dispersity / heterogeneity of the samples.

Finally, our study revealed a robust assessment of the gross conformational properties with classical scaling relationships (Fig. 6) and the calculation of the individual statistical macromolecular chain parameters including Kuhn length and diameter of the macromolecular chains (Fig. 7). All of these results are supported by the straightforward conformation zoning approach (Fig. 8).

While exemplified by CMCs, for future studies, there is practically no roadblock for a self-sufficient solution characterization of any disperse macromolecule population in solution including data from hydrodynamic and light scattering techniques. Even only one of those techniques is available, it is advisable to report as many as possible characteristics associated to such macromolecules. Those information may later enable revisiting such data with other literature or documentation in terms of quality control purposes and the established structure-property relationships.

Acknowledgments

The authors acknowledge support of this study from the Thüringer Ministerium für Wirtschaft, Wissenschaft und Digitale Gesellschaft (TMWWDG, ProExzellenz II, NanoPolar) for funding the Solution Characterization Group (SCG) at the Jena Center for Soft Matter (JCSM), Friedrich Schiller University Jena. I.P. is grateful for the support by a grant from the Russian Science Foundation (project No 16-13-10148). This work was financially supported by the DFG-funded Collaborative Research Center PolyTarget (SFB 1278, projects Z01 and A02).

Appendix A. Supplementary data

Supplementary material related to this article can be found, in the online version, at doi:https://doi.org/10.1016/j.carbpol.2019.115452.

References

Aravamudhan, A., Ramos, D. M., Nada, A. A., & Kumbar, S. G. (2014). *Natural polymers: Polysaccharides and their derivatives for biomedical applications.* 67–89.
Arinaitwe, E., & Pawlik, M. (2014). Dilute solution properties of carboxymethyl celluloses of various molecular weights and degrees of substitution. *Carbohydrate Polymers, 99*, 423–431.
Brown, W., & Henley, D. (1964). Studies on cellulose derivatives. *Die Makromolekulare Chemie, 79*(1), 68–88.
Chaturvedi, S. K., Ma, J., Brown, P. H., Zhao, H., & Schuck, P. (2018). Measuring macromolecular size distributions and interactions at high concentrations by sedimentation velocity. *Nature Communications, 9*(1), 4415.
Davis, R. M. (1991). Analysis of dilute solutions of (carboxymethyl)cellulose with the electrostatic wormlike chain theory. *Macromolecules, 24*(5), 1149–1155.
Debye, P. (1947). Molecular-weight determination by light scattering. *The Journal of Physical and Colloid Chemistry, 51*(1), 18–32.
Gray, H. B., Jr, Bloomfield, V. A., & Hearst, J. E. (1967). Sedimentation coefficients of linear and cyclic wormlike coils with excluded-volume effects. *The Journal of Chemical Physics, 46*(4), 1493–1498.
El-Hag Ali, A., Abd El-Rehim, H. A., Kamal, H., & Hegazy, D. E. S. A. (2008). Synthesis of carboxymethyl cellulose based drug carrier hydrogel using ionizing radiation for possible use as site specific delivery system. *Journal of Macromolecular Science, Part A, 45*(8), 628–634.
Eremeeva, T. E., & Bykova, T. O. (1998). Sec of mono-carboxymethyl cellulose (cmc) in a wide range of ph; mark–houwink constants. *Carbohydrate Polymers, 36*(4), 319–326.
Fessler, J. H., & Ogston, A. G. (1951). Studies of the sedimentation, diffusion and viscosity of some sarcosine polymers in aqueous solution. *Transactions of the Faraday Society, 47*, 667.
Fujita, H. (1956). Effects of a concentration dependence of the sedimentation coefficient in velocity ultracentrifugation. *The Journal of Chemical Physics, 24*(5), 1084–1090.
Fujita, H., Hutchinson, E., & Van Rysselberghe, P. (2016). *Mathematical theory of sedimentation analysis.* Elsevier Science.
Grube, M., Leiske, M. N., Schubert, U. S., & Nischang, I. (2018). Pox as an alternative to peg? A hydrodynamic and light scattering study. *Macromolecules, 51*(5), 1905–1916.
Harding, S. E. (1995). On the hydrodynamic analysis of macromolecular conformation. *Biophysical Chemistry, 55*(1–2), 69–93.
Harding, S. E., Adams, G. G., Almutairi, F., Alzahrani, Q., Erten, T., Kok, M. S., & Gillis, R. B. (2015). Ultracentrifuge methods for the analysis of polysaccharides, glycoconjugates, and lignins. *Methods in Enzymology, 562*, 391–439.
Heinze, T., & Koschella, A. (2005). Carboxymethyl ethers of cellulose and starch - A review. *Macromolecular Symposium, 223*, 13–39.
Heinze, T., & Pfeiffer, K. (1999). Studies on the synthesis and characterization of carboxymethylcellulose. *Die Angewandte Makromolekulare Chemie, 266*(1), 37–45.
Heinze, T., Erler, U., Nehls, I., & Klemm, D. (1994). Determination of the substituent pattern of heterogeneously and homogeneously synthesized carboxymethyl cellulose by using high-performance liquid chromatography. *Angewandte Makromolekulare Chemie, 215*(1), 93–106.
Hollabaugh, C. B., Burt, L. H., & Walsh, A. P. (1945). Carboxymethylcellulose. Uses and applications. *Industrial & Engineering Chemistry, 37*(10), 943–947.
Johnston, J. P., & Ogston, A. G. (1946). A boundary anomaly found in the ultracentrifugal sedimentation of mixtures. *Transactions of the Faraday Society, 42*, 789.
Kamide, K., Saito, M., & Suzuki, H. (1983). Persistence length of cellulose and cellulose derivatives in solution. *Die Makromolekulare Chemie, Rapid Communications, 4*(1), 33–39.
Kim, G. T., Jeong, S. S., Joost, M., Rocca, E., Winter, M., Passerini, S., & Balducci, A. (2011). Use of natural binders and ionic liquid electrolytes for greener and safer lithium-ion batteries. *Journal of Power Sources, 196*(4), 2187–2194.
Klemm, D., Heublein, B., Fink, H. P., & Bohn, A. (2005). Cellulose: Fascinating biopolymer and sustainable raw material. *Angewandte Chemie, 44*(22), 3358–3393.
Lavrenko, P. N., Okatova, O. V., Dauttsenberg, K., & Filipp, B. (1991). Diffusion and sedimentation of monosubstituted carboxymethyl cellulose in deca-diluted aqueous cadoxene. *Polymer Science U.S.S.R. 33*(5), 937–944.
Lavrenko, P. N., Okatova, O. V., Dautzenberg, H., & Philipp, B. (1993). Molecular inhomogeneity of carboxymethyl cellulose from fractionation and sedimentation-velocity data. *Cellulose Chemistry and Technology, 27*(5), 469–476.
Lavrenko, P. N., Okatova, O. V., Tsvetkov, V. N., Dautzenberg, H., & Philipp, B. (1990). Conformation of carboxymethylcellulose in cadoxen-water solutions. *Polymer, 31*(2), 348–352.
Lavrenko, P. N., Okatova, O., & Dautzenberg, H. (1999). *Inhomogeneity and conformational parameters of low-substituted carboxymethyl cellulose from analytical ultracentrifugation data.* Berlin, Heidelberg: Springer Berlin Heidelberg192–200.
Lebowitz, J., Lewis, M. S., & Schuck, P. (2002). Modern analytical ultracentrifugation in protein science: A tutorial review. *Protein Science, 11*(9), 2067–2079.
Lee, B.-R., & Oh, E.-S. (2013). Effect of molecular weight and degree of substitution of a sodium-carboxymethyl cellulose binder on $li_4ti_5o_{12}$ anodic performance. *The Journal of Physical Chemistry C, 117*(9), 4404–4409.

Li, H. Y., Song, X., & Seville, P. C. (2010). The use of sodium carboxymethylcellulose in the preparation of spray-dried proteins for pulmonary drug delivery. *European Journal of Pharmaceutical Sciences, 40*(1), 56–61.
Li, J., Lewis, R. B., & Dahn, J. R. (2007). Sodium carboxymethyl cellulose. *Electrochemical and Solid-State Letters, 10*(2), A17.
Lichtenthaler, F. W. (2007). *Carbohydrates as renewable raw materials: A major challenge of green chemistry. Methods and reagents for Green chemistry: An introduction*23–63.
Lichtenthaler, F. W., & Peters, S. (2004). Carbohydrates as green raw materials for the chemical industry. *Comptes Rendus Physique, 7*(2), 65–90.
Lühmann, T., Schmidt, M., Leiske, M. N., Spieler, V., Majdanski, T. C., Grube, M., ... Meinel, L. (2017). Site-specific poxylation of interleukin-4. *ACS Biomaterials Science & Engineering, 3*(3), 304–312.
Luna-Martínez, J. F., Hernández-Uresti, D. B., Reyes-Melo, M. E., Guerrero-Salazar, C. A., González-González, V. A., & Sepúlveda-Guzmán, S. (2011). Synthesis and optical characterization of zns–sodium carboxymethyl cellulose nanocomposite films. *Carbohydrate Polymers, 84*(1), 566–570.
Mijnlieff, P. F., & Jaspers, W. J. M. (1971). Solvent permeability of dissolved polymer material. Its direct determination from sedimentation measurements. *Transactions of the Faraday Society, 67*, 1837.
Murodov, E. A., Urinov, E. U., & Turaev, A. S. (2018). Molecular weight and conformational characteristics of carboxymethyl cellulose and its nitroesters. *International Polymer Science and Technology, 32*(12), 62–65.
Nadagouda, M. N., & Varma, R. S. (2007). Synthesis of thermally stable carboxymethyl cellulose/metal biodegradable nanocomposites for potential biological applications. *Biomacromolecules, 8*(9), 2762–2767.
Nasatto, P., Pignon, F., Silveira, J., Duarte, M., Noseda, M., & Rinaudo, M. (2015). Methylcellulose, a cellulose derivative with original physical properties and extended applications. *Polymers, 7*(5), 777–803.
Nischang, I., Perevyazko, I., Majdanski, T., Vitz, J., Festag, G., & Schubert, U. S. (2017). Hydrodynamic analysis resolves the pharmaceutically-relevant absolute molar mass and solution properties of synthetic poly(ethylene glycol)s created by varying initiation sites. *Analytical Chemistry, 89*(2), 1185–1193.
Oberlerchner, J. T., Rosenau, T., & Potthast, A. (2015). Overview of methods for the direct molar mass determination of cellulose. *Molecules, 20*(6), 10313–10341.
Okatova, O. V., Lavrenko, P. N., & Dautzenberg, H. (2000). Hydrodynamic properties and conformational characteristics of low-substituted carboxymethyl cellulose in solution. *Polymer Science Series A - Springer, 42*(7), 736–742.
Pavlov, G. M. (1996). The concentration dependence of sedimentation for polysaccharides. *European Biophysics Journal*.
Pavlov, G. M., & Frenkel, S. Y. (1983). Sedimentation velocity of dilute and moderately concentrated solutions of cellulose nitrate. *Polymer Science U.S.S.R. 25*(5), 1173–1179.
Pavlov, G. M., Perevyazko, I., Okatova, O. V., & Schubert, U. S. (2011). Conformation parameters of linear macromolecules from velocity sedimentation and other hydrodynamic methods. *Methods, 54*(1), 124–135.
Pavlov, G. M., Rowe, A. J., & Harding, S. E. (1997). Conformation zoning of large molecules using the analytical ultracentrifuge. *Trends in Analytical Chemistry, 16*(7), 401–405.
Pohl, M., Morris, G. A., Harding, S. E., & Heinze, T. (2009). Studies on the molecular flexibility of novel dendronized carboxymethyl cellulose derivatives. *European Polymer Journal, 45*(4), 1098–1110.
Ramesh, H. P., & Tharanathan, R. N. (2003). Carbohydrates–the renewable raw materials of high biotechnological value. *Critical Reviews in Biotechnology, 23*(2), 149–173.
Rinaudo, M., Danhelka, J., & Milas, M. (1993). A new approach to characterising carboxymethylcelluloses by size exclusion chromatography. *Carbohydrate Polymers, 21*(1), 1–5.
Saake, B., Horner, S., Kruse, T., Puls, J., Liebert, T., & Heinze, T. (2000). Detailed investigation on the molecular structure of carboxymethyl cellulose with unusual substitution pattern by means of an enzyme-supported analysis. *Macromolecular Chemistry and Physics, 201*(15), 1996–2002.
Schuck, P. (2000). Size-distribution analysis of macromolecules by sedimentation velocity ultracentrifugation and lamm equation modeling. *Biophysical Journal, 78*(3), 1606–1619.
Schulz, V. G. V., & Penzel, E. (1968). Expansionskoeffizient (α) und zweiter virialkoeffizient (a2) der lösungen von cellulosetrinitraten in aceton. *Die Makromolekulare Chemie, 112*(1), 260–280.
Shakun, M., Maier, H., Heinze, T., Kilz, P., & Radke, W. (2013). Molar mass characterization of sodium carboxymethyl cellulose by sec-malls. *Carbohydrate Polymers, 95*(1), 550–559.
Sitaramaiah, G., & Goring, D. A. I. (1962). Hydrodynamic studies on sodium carboxymethyl cellulose in aqueous solutions. *Journal of Polymer Science, 58*(166) 1107-&.
Svedberg, T., & Sjögren, B. (1930). The molecular weights of amandin and of excelsin. *Journal of the American Chemical Society, 52*(1), 279–287.
Tsvetkov, V. N. (1989). *Rigid-chain polymers: Hydrodynamic and optical properties in solution.* Springer.
Tsvetkov, V. N., Lavrenko, P. N., & Bushin, S. V. (1984). Hydrodynamic invariant of polymer molecules. *Journal of Polymer Science: Polymer Chemistry Edition, 22*(11), 3447–3486.
Wales, M., & Van Holde, K. E. (1954). The concentration dependence of the sedimentation constants of flexible macromolecules. *Journal of Polymer Science, 14*(73), 81–86.
Wyatt, P. J. (1993). Light scattering and the absolute characterization of macromolecules. *Analytica Chimica Acta, 272*(1), 1–40.
Yamakawa, H., & Fujii, M. (1973). Translational friction coefficient of wormlike chains. *Macromolecules, 6*(3), 407–415.